Evaluation of high-resolution precipitation analyses using a dense station network

A. Kann[1], I. Meirold-Mautner[1], F. Schmid[1], G. Kirchengast[2], J. Fuchsberger[2] , V. Meyer[1], L. Tüchler[1], and B. Bica[1]

[1]{Department of Forecasting Models, Central Institute for Meteorology and Geodynamics (ZAMG), Vienna, Austria}

[2]{Wegener Center for Climate and Global Change (WEGC) and Institute for Geophysics, Astrophysics, and Meteorology/Institute of Physics (IGAM/IP), University of Graz, Graz, Austria}

Correspondence to: A. Kann (alexander.kann@zamg.ac.at)

Abstract

The ability of radar-rain gauge merging algorithms to precisely analyse convective precipitation patterns is of high interest for many applications, e. g. hydrological modelling, thunderstorm warnings, and, as a reference, to spatially validate numerical weather prediction models. However, due to drawbacks of methods like cross-validation and due to the limited availability of reference datasets on high temporal and spatial scale, an adequate validation is usually hardly possible, especially on an operational basis. The present study evaluates the skill of very high resolution and frequently updated precipitation analyses (rapid-INCA) by means of a very dense weather station network (WegenerNet), operated in a limited domain of the south-eastern parts of Austria (Styria). Based on case studies and a longer term validation over the convective season 2011, a general underestimation of the rapid-INCA precipitation amounts is shown by both continuous and categorical verification measures, although the temporal and spatial variability of the errors is - by convective nature - high. The contribution of the rain gauge measurements to the analysis skill is crucial. However, the capability of the analyses to precisely assess the convective precipitation distribution predominantly depends on the representativeness of the stations under the prevalent convective condition.

1 Introduction

Reliable precipitation analyses and forecasts with both high temporal update frequency and high spatial resolution are essential for many applications. For example, hydrological models usually require gridded precipitation fields on small scales and short lead times which form the major component of flood warning systems (Komma et al., 2007). In climate research, precipitation re-analyses performed over decades are employed to estimate return periods or other extreme value statistics and often are of high social and economic relevance. Gridded precipitation analyses are also gaining importance in the field of spatial verification of numerical weather prediction (NWP) models, especially since convection-resolving models allow for simulating small-scale convective storms.

A variety of methods exists which aim at generating realistic and skillful precipitation analyses. Goudenhoofdt and Delobbe (2009) have shown that the combination of both radar derived precipitation estimates and rain gauge measurements is superior to the individual fields because particular strengths are emphasized, and weaknesses are compensated. Although it is unquestionable that generally, such combination methods improve the skill of quantitative precipitation analysis, their results strongly depend on the precipitation character, the local environment (e.g. orography), the quality of the radar and rain gauge data, the scale of interest (e.g. for catchment size scales) and the respective application of the precipitation analysis (Rossa et al., 2005). Thus, the impact on validation results of NWP models can be large and should be taken into account (Rezacova and Sokol, 2002) depending on e.g. the radar-rain gauge combination scheme and the diverse application fields. An overview of radar-rain gauge merging algorithms has been elaborated within the COST 717 project (Rossa et al., 2005), some of them employ bias adjustments schemes (Pereira et al., 1998; Chumchean et al., 2006; Overeem et al., 2009), Kriging approaches (Krajewski, 1987; Sun et al., 2000) also including Bayesian techniques (Handcock and Stein, 1993) and regression-type algorithms (Gregow et al., 2013). A few merging algorithms are of multi-source nature, including radar and rain gauge data and additional components like NWP data to improve the analysis skill (e.g. NIMROD system by Golding (1998); INCA system by Haiden et al. (2011)).

The Integrated Nowcasting through Comprehensive Analysis (INCA) system has been developed at the Central Institute for Meteorology and Geodynamics in Vienna, Austria (ZAMG) and is in operational use since spring 2004. Besides precipitation (the most

traditional nowcasting parameter) many different parameters are computed by INCA (e.g. precipitation type, temperature, humidity, wind etc.). The techniques for computing analyses and nowcasts vary from parameter to parameter, as well as temporal resolution and update frequency.

A common way of validating the skill of precipitation analyses is the method of leave-one-out cross-validation. However, this method has drawbacks: It is computationally expensive, it assumes a random distribution of the stations with respect to climatology and topography, the results depend on the local conditions of the stations, and - due to the often inhomogeneous and sparse station networks - small-scale features are usually not captured.

Due to its limited representativeness, traditional point-wise verification against station measurements is not adequate and is amended by spatial verification methods like the Structure-Amplitude-Location (SAL) method (Wernli et al., 2008). These novel verification methods require gridded precipitation analyses, preferably model-independent, of high quality as a reference. Wittmann et al. (2010) have used high resolution precipitation analyses to validate the skill of different limited area models (LAM) during a convective season. Similarly, Sattler and Feddersen (2005) have applied daily precipitation analyses to evaluate the quality of a limited area and a global ensemble system during heavy precipitation events.

In the present article, the INCA precipitation analyses are validated against the independent dataset of the WegenerNet climate station network (operated by the Wegener Center for Climate and Global Change, University of Graz, Austria; (Kirchengast et al., 2014)). Rather than the development of new verification measures, this article applies well-established verification standards (e.g. cross-validation and feature-based metrics) based on this dense station network. The WegenerNet dataset has already been successfully applied to validate temperature, humidity, and wind speed analyses in an operational context (Kann et al., 2011). Furthermore, the dense station network allows for a thorough evaluation of INCA precipitation for small-scale, convective precipitation patterns.

Section 2 introduces the rapid-INCA analysis module and the station network WegenerNet. Section 3 briefly illustrates the synoptic conditions of selected cases with heavy precipitation in August and September 2011, and their skill scores of verification. Section 4 describes the results of a long-term validation during the whole convective period from April to September 2011, followed by a conclusion.

2 Data and methods

2.1 The rapid-INCA precipitation analysis

The rapid-INCA system is an extension of INCA, specifically developed for precipitation nowcasting with a 5-minute accumulation period and update frequency (in contrast to 15 minutes in the original INCA version). Radar data from the Austrian weather radar network as well as measurements from the Austrian automatic weather stations network (Teilautomatische Wetterstationen, TAWES) are available every five minutes and therefore allow for rapid-INCA updates at this frequency. In situations with rapidly changing weather conditions, such as fast developing thunderstorms, rapid-INCA is a helpful tool (both, in analysis and nowcasting mode) as it provides new assessments of the spatial precipitation distribution every five minutes. However, the focus of the present study is on the rapid-INCA analysis procedure, not on nowcasting.

The rapid-INCA precipitation algorithm merges rain gauge measurements from approximately 270 TAWES stations with radar derived precipitation estimates. The synthesis is designed to combine the strengths of both data sources, i.e. the quantitative accuracy of the station measurements and the detailed spatial information of the radar image. However, the algorithmic synthesis has also to cope with the weaknesses and error sources of both measurement methods and – as far as possible – to compensate for them. These weaknesses are predominantly the potentially low representativeness of site-specific measurements and the general quantitative uncertainty of precipitation estimates from radar reflectivity.

The precipitation analysis consists of the following steps (cf. Haiden et al. (2011) for a detailed description):

1. Radar derived quantitative precipitation estimates (QPE): The Austrian radar network consists of two lowland and three mountain radar stations operated by the Austrian aviation service (Austro Control). Each radar scans the atmosphere in 5-minute intervals with 16 customized elevation angles up to an angle of 67° and to a range of 224 km. A MaxCAPPI (Maximum Constant Altitude Plan Position Indicator) product is provided for each radar station, which is computed from three-dimensional radar volumes by projecting the maximum value within a vertical column to a two-dimensional plane. The data are ground clutter corrected by Doppler processing and multi-temporal/multi-parameter

statistical filters. No further correction on the beam is done, therefore radar data derived products may be influenced by measurement errors, such as bright band, signal attenuation, scan strategy, radar miscalibration, radome wetting, and errors due to non-meteorological echoes. The MaxCAPPI data are provided on a Cartesian grid with a horizontal resolution of 1 km and reduced to 14 reflectivity classes ('no rain', 11.8, 14.0, 19.5, 22.0, 26.7, 30.0, 34.2, 38.0, 41.8, 46.0, 50.2, 54.3, 58.0 [dBZ]). Reflectivities are operationally converted to rainfall intensities by using the Marshall-Palmer relation $Z = 200\ R^{1.6}$ (Marshall and Palmer, 1948). Further details about the radar stations and specifications can be found in Kaltenboeck (2012) and Kaltenboeck and Steinheimer (2014). At ZAMG, for lack of radial data, a pattern recognition filter is applied on the MaxCAPPI data to correct R-LAN signals. As the data are only corrected for ground clutter and R-LAN, beside residual clutter, all other error sources have to be considered when radar QPE is used. These errors are reflected in the MaxCAPPI data. As in the MaxCAPPI calculation always the maximum value of a vertical column is used, especially bright band effects in stratiform rain and the hail core in thunderstorms lead to overestimated rainfall intensities. Other important aspects are partial and total beam shielding and beam broadening with increasing distance to the radar station. In the target region the minimum height which is seen by the radar network is around 2000 m above ground (Figure 2b). Rainfall close to the ground, which is measured by ground stations, is not captured in the radar signals, so that potential rainfall intensification or evaporation processes and size sorting due to wind shear on the way to the ground are missed. Furthermore, with the closest radar stations at distances of approx. 100 km (the mountain site Zirbitzkogel) and approx. 135 km (lowland site Rauchenwarth) the 1° beam widths become as broad as 1.7 km and 2.35 km, respectively. The large radar bin volumes, together with the high variability of precipitation in space and time, potentially lead to inhomogeneous beam-filling problems and unrepresentative precipitation values. Finally, the fixed Z-R relationship, which does not take into account the variety of different drop-size distributions, and the restricted data resolution of 14 intensity classes are further considerable limitations for radar-predicted rainfall intensities. Still, the MaxCAPPI product is the best available data source for INCA. With all the restrictions of radar-based QPE, radar data have the advantage to capture the precipitation structure in general, so that this information may be added to the local point measurements. INCA reads the MaxCAPPI data provided by each radar and generates a composite by selecting the

highest value at each grid point. The MaxCAPPI composite is bi-linearly interpolated onto the INCA grid. A pre-scaling of the radar data is conducted before a high quality analysis can be calculated as precipitation estimates of the radar may underlie important systematic errors. The local scaling factor results from the ratio of monthly precipitation sums of station interpolation to monthly precipitation sums of radar derived QPE. To avoid unrealistically high scaling factors a maximum value of 2 is set. In addition to the fixed scaling, a latest-data scaling procedure is applied using recent radar and observation data.

2. Interpolation of rain gauge data: The 1-minute measurements are aggregated to 5-minute sums and interpolated by inverse-distance weighting (IDW) onto the 1km INCA grid by using the eight nearest stations. Note that only those measurements are used which fulfill several quality control criteria including time-series control, comparison with radar data and with neighboring stations. Figure 2 shows the operational rapid-INCA domain and the distribution of automatic stations as well as the position of the five radar locations.
3. Combination of weather station interpolation and re-scaled radar field: The combined field is generated by a weighted relation between both fields and leads to a better precipitation distribution in space than each individual field. It is assured that the observed measurement at the station location is reproduced (within the resolution limits). The larger the distance to the stations, the higher are the weights of the (scaled) radar field. On the other hand, lower radar data quality due to topographic shielding gives higher weight to the interpolated station data. Additionally, elevation effects are parameterized accounting for the increase of precipitation amounts with height (Haiden and Pistotnik, 2009). Figure 3 illustrates the combination algorithm in the case of 13 September 2014, 02:40 UTC. In areas with low radar quality, the combination algorithm assigns large weights to the station interpolation. The radar derived QPE contributes with small-scale convective cells which were not captured by TAWES stations of ZAMG.

2.2 The WegenerNet

This brief description of the station network WegenerNet, operated by the Wegener Center for Climate and Global Change of the University of Graz, Austria, is based on Kirchengast et al. (2014) and Kabas (2012), wherein detailed further information can be found. The WegenerNet comprises 151 meteorological stations within an area of about 20 km × 15 km in southeastern Styria, Austria (centered near the city of Feldbach, 46.93°N, 15.90°E), a region

with high weather variability (Kabas et al., 2011a, 2011b). The stations are arranged on a quasi-regular 1.4 km × 1.4 km grid (Figure 1) and measure the parameters air temperature, relative humidity, and precipitation amount. Selected stations additionally provide measurements of wind and soil parameters. Furthermore, air pressure and net radiation are observed at one reference station. The collected data are processed by the automatic WegenerNet Processing System (WPS). The raw data are stored by Internet loggers (GeoPrecision GmbH, Germany; www.geoprecision.com) and transferred via GPRS to the database at the Wegener Center Graz. The GPRS transmission is performed hourly, with subsets of about 30 stations transferring in stacked 5-minute batches during the first half of the hour.

The incoming data files are stored in a database and are checked by the Quality Control System (QCS). The QCS is run hourly and it checks for each of the 151 stations the availability and correctness as well as the technical and physical plausibility of the measured data in eight quality-control (QC) layers (Table 1).

QC layers 0 and 1 check for data availability, QC layers 2, 5, and 7 are fairly common types of checks, on bounds and deviations, whereas the inter-station check of QC layer 6, which is made to detect implausible "jumps" of parameter values between stations, is unique to this type of dense station grid. For precipitation data, layers 2, 4, 5, and 6 are key: Layer 2 checks for rain rates exceeding sensor specifications, in layer 4 rain rates higher than climatological bounds are detected, and layer 5 looks for inconsistencies between rain gauges at a single station. Layer 6 is able to detect partially or totally blocked funnels, flushes due to sudden opening of blocked funnels, and in general unusual deviations from the values at neighboring stations. If all QC layers are passed without any detection, the data receive a QC flag of 0, indicating the highest quality. In the present study, only such flag 0 data were used. Further details about the QCS and all implemented checks can be found in Kirchengast et al. (2014) and Scheidl (2014).

In the Data Product Generator, gridded data of the main parameters are derived on a regular 200 m × 200 m Universal Transverse Mercator (UTM) grid from individual station measurements by IDW. Subsequently, station data and gridded data (at 5-minute resolution) are also averaged (summed up for precipitation) to various weather and climate data products (from half-hourly up to annual).

For application purposes the resulting data and further information on the station network are available for users at the WegenerNet data portal (www.wegenernet.org) in near-real time (data latency less than 30 minutes to 90 minutes). The WegenerNet provides highly resolved individual station data and regular grids since 01 January 2007 as a new data source for research projects investigating local-scale weather and climate and environmental change. Moreover, the data records serve as information source for various applications in the study region (Kirchengast et al., 2014; Kabas et al., 2011b).

2.3 Method

The WegenerNet measurements (5-minute precipitation sums) serve as reference in the present study and thus most of the standard comparison techniques are carried out at these station locations. The INCA related fields, rapid-INCA analyses, radar derived QPE and rain gauge measurements (TAWES), are interpolated bi-linearly from the 1 km x 1 km INCA grid to the WegenerNet station locations. This interpolation method has been chosen, because the WegenerNet grid is nearly regular with a spatial resolution comparable to the rapid-INCA grid resolution.

Besides bias, mean absolute error (MAE) and root mean squared error (RMSE), the skill scores Equitable Thread Score (ETS), True Skill Score (TSS) and Frequency Bias Index (FBI), which are commonly used for validating precipitation, have been computed for a threshold of 0.5 mm per 5 minutes (Table 2).

For spatial comparisons, IDW interpolation has been applied to obtain WegenerNet measurements on the INCA grid. A quadratic distance weighting function has been chosen by taking into account the five nearest neighbors as the station density of WegenerNet in the target region is relatively high and the respective observations should not be smoothed too much. The resulting field has been processed to obtain the spatial verification indicators structure, amplitude and location (SAL; Wernli et al., 2008), but also to demonstrate the spatial patterns of standard verification measures.

3 Heavy precipitation case studies

For the selection of cases with heavy precipitation during the convective season of 2011 the definition of Wussow (1922) for integration times smaller than 30 minutes has been followed:

$$h_n \geq \sqrt{5t - \left(\frac{t}{24}\right)^2}, \qquad (1)$$

where t is the time in minutes and h_n the amount of precipitation in millimeter. Thus, a heavy precipitation event is characterized by precipitation amounts exceeding 5 mm in 5 minutes, 7 mm in 10 minutes or 12 mm in 30 minutes.

3.1 Synoptic situations

Four cases with heavy precipitation over the WegenerNet region were selected. Figure 4 shows 2-hour sums of the 5-minute rapid-INCA analyses of these selected cases. The synoptic situation for each of the cases is illustrated in Figure 5.

- 03 August 2011, 21:00 UTC - 23:00 UTC

  A trough northwest of Ireland and high pressure centered over the Baltics bring a warm upper-level flow from the southwest into Austria. At 18:00 UTC an eastwards-propagating ridge in relative topography (represented by the orange line in Figure 5, top left) indicates high values of temperature and humidity in the south-eastern part of Austria. CAPE values in the WegenerNet area amount to more than 2000 J/kg and the lifted index (LI) is around -6 K, thus indicating a potential for convective developments. A convergence line gradually approaches from the west and leads to the formation of thunderstorms in the western alpine regions of Austria but also in the south-eastern parts of the country.

- 15 August 2011, 15:00 - 17:00 UTC

  The surface pressure analysis at 12:00 UTC (Figure 5, top right) shows a low pressure system centered over Iceland, with secondary lows over southern Sweden and Ireland, whereas rather high pressure and weak gradients prevail over large parts of central Europe. A cold front associated with the trough over southern Sweden crosses Austria in the course of the day. At 15:00 UTC, INCA temperature analyses show

temperatures above 30°C in the easternmost parts of Austria (33° in western Hungary) and below 16° only a few kilometers west of the WegenerNet. A few hours ahead of the event, Deep Layer Shear (DLS) values range to approximately 12 m/s according to the 03:00 UTC sounding at 40 km-distant station 'Graz Thalerhof' (WMO ID 11240). CAPE (2000 J/kg) and LI (-4 K) values at 15:00 UTC are highest within the Alpine region.

- 19 August 2011, 13:00 - 15:00 UTC

  A cold front associated with a low over the southern Baltic Sea approaches the northern Alpine rim from the northwest (Fig. 5, bottom left), with its forward motion being gradually decreased. Nevertheless cold air is advected in higher levels, whereas a northerly low level jet with a maximum in 925 hPa brings warm moist air into the target area. Thunderstorms were widespread on that day. In the vicinity of the WegenerNet, DLS values were around 10 m/s and CAPE close to 1400 J/kg in the afternoon.

- 01 September 2011, 16:00 - 18:00 UTC

  A very shallow surface pressure distribution with weak frontal signals dominates over most parts of Central and Eastern Europe. The air mass over the WegenerNet was generally moist and unstable with an increased potential for convective developments (LI around -4 K, DLS=12 m/s). The thunderstorm initiation might be attributed to a recent crossing of a weak warm front in northerly direction: In the warm sector the advection of warm air aloft is gradually cut off while the forcing at the ground is given through radiative heating.

3.2 5-minute rapid-INCA analyses for the selected cases

Figure 6 shows the spatio-temporal distribution of 5-minute rapid-INCA precipitation analyses in the region of the WegenerNet which is indicated by the black rectangle. On 03 August 2011, the maximum precipitation amounts are between 2 and 3 mm per 5 min at 22:05 UTC, and then decrease with time. The precipitation cells on 15 August 2011 are gradually expanded and intensified with time to 6 mm per 5 min. On 19 August 2011, a heavy precipitation cell moves slowly across the northern part of the WegenerNet area, and on 01 September 2011, extremely high precipitation amounts are reached (>10 mm/5 min) before the precipitation cells leave the WegenerNet domain to the south-east.

3.3 Time series and verification of rapid-INCA analyses for the selected cases

The precipitation rates (per five minutes) of WegenerNet measurements, rapid-INCA, radar derived QPE, and TAWES station measurements have been averaged over the WegenerNet domain to show the temporal evolution of the precipitation cells in the four selected cases (Figure 7). Within the WegenerNet area, only two TAWES stations are located (see Figure 1) and contribute to the interpolated stations field. Predominantly, both the onset and evolution of rapid-INCA precipitation amounts follow the WegenerNet observations. However, rapid-INCA underestimates the average precipitation rate in three of the cases, and shows an earlier onset and overestimation in the last case (01 September 2011). The latter situation is triggered by a slight overestimation of radar derived QPE.

On the first three example days, widespread rain systems with embedded intensified precipitation regions and convection cross the target region from south-west/west. In these cases, signal attenuation in the extensive rain regions between radar station and target region and wetted radomes can contribute to the underestimated rain intensities in the radar QPE. On 01 September 2011, mainly one intense thunderstorm with severe hail at the ground is observed crossing the target region. The rainfall overestimation in this case may be attributed to uncorrected hail signals while the signal attenuation is negligible. Even if this simple validation approach is not suitable for a detailed quantitative analysis, it gives a qualitative view of the four cases under investigation.

The verification measures relative bias, MAE, and RMSE (scaled by the mean observed precipitation at each of the WegenerNet stations) have been computed and averaged over space to evaluate the error characteristics of rapid-INCA. Only time steps with a minimum observed precipitation of 0.1mm/5min have been selected for the computations. Figure 8 shows the resulting error measures along with the standard deviation indicated by the error bars. A negative bias is visible for all rapid-INCA constituents except for the TAWES station interpolation on 15 August 2011. This is in accordance with the findings in Figure 7. The error measures MAE and RMSE are similar for rapid-INCA and radar derived QPE, indicating that the radar derived QPE errors predominantly contribute to the rapid-INCA analysis errors. In certain cases (e.g. 15 August 2011 and 01 September 2011), the rapid-INCA analysis error is larger than the radar derived QPE error. It indicates that the inclusion of the TAWES station observations may decrease the skill, i.e. the TAWES station observations are not representative for this specific precipitation event.

Moreover, the variation in the error measures across the WegenerNet domain is large for the TAWES stations, specifically on 15 August 2011 (only two TAWES stations are located within the WegenerNet area and constitute the interpolated stations field; see Figure 1). The comparison with the WegenerNet stations results in high variability of bias, MAE, and RMSE on 15 August 2011 and 01 September 2011, which demonstrates the low representativeness of the TAWES station field. In such cases, the rapid-INCA analysis (i.e. combination of station interpolation and radar derived QPE) yields worse error measures than the pure radar derived QPE. The high variability of rain gauge measurements (TAWES) can also be seen in the spatio-temporal distribution as shown in Figure 9. The two TAWES stations are hit by a heavy (localized) precipitation cell on 01 September 2011 at 16:45 UTC, and the interpolation results in an exaggeration of the precipitation field (compared to the rapid-INCA analysis in Figure 6). In this case, an IDW interpolation with an exponent higher than 2 (instead of $1/r^2$), would limit the spatial influence of the TAWES stations and improve the results in regimes with local convection.

Averaged skill scores, FBI, TSS, and ETS, (for a threshold of 0.5 mm/5 min at WegenerNet stations) are shown in Figure 10. In the case of low representativeness of the TAWES station interpolation (01 September 2011), the scores FBI and ETS from radar derived QPE yield better values than those of rapid-INCA. Hence, the station contribution is decreasing the skill. However, in the majority of cases, the skill of rapid-INCA is higher than of pure radar derived QPE. Higher thresholds than 0.5 mm/5 min lead to worse results of the scores which can partly be explained by the decreasing sample size. Another reason might be the tendency to miss heavy precipitation events with rapid-INCA.

For an objective analysis of the four cases, we applied the Structure-Amplitude-Location (SAL) method (Wernli et al., 2008) to each time step within the respective 2-hour intervals. The results are averaged and plotted in Figure 11 with error bars indicating the standard deviation of the SAL time series. As already emphasized in previous figures, the amplitude values of rapid-INCA show an underestimation of the observed precipitation in all but one case. Radar derived QPE exhibits a higher underestimation than rapid-INCA which demonstrates the positive effect of merging interpolated rain gauge measurements (TAWES) with data of radar QPE. Only on 01 September 2011 did the TAWES station data significantly overestimate precipitation, and in turn over-compensate the radar derived QPE underestimation to finally yield a positive amplitude value of rapid-INCA. Positive structure

values indicate too large and/or too flat precipitation cells. rapid-INCA overestimates the extent of precipitation cells (on average, as does the TAWES station interpolation). Radar derived QPE in contrast yields negative structure values, and thus underestimates the extent of the cells. These results suggest that the interpolation method of rain gauge measurements (TAWES) should take into account the current convective situation to be more confined for cases of heavy precipitation (e.g. IDW with a higher exponent, or more sophisticated interpolation methods such as Kriging by using radar data fingerprints).

The location indicator of Figure 11 does not yield conclusive results as it is relatively low for each of the rapid-INCA constituents. This behavior may be explained by the small area under investigation and thus limited errors in displacement of cells.

4 Long-term validation results using WegenerNet data as reference

For the long-term validation, rapid-INCA analyses, radar derived QPE, and interpolated TAWES station measurements from the convective season in 2011 (01 April 2011 to 30 September 2011) at 5-minute time steps have been interpolated to the WegenerNet stations (see section 2.3). The relative bias, MAE, and RMSE (scaled by mean measured WegenerNet precipitation) have been computed for each of the WegenerNet stations and, for better spatial representation, interpolated to the INCA domain (by IDW).

Only time steps with measured WegenerNet precipitation exceeding a certain threshold have been used to avoid falsifying the error measures with precipitation-free time steps. The Figure 12 presents the results for a selected threshold of 0.5 mm/5 min.

The bias shows substantial underestimation of the radar derived QPE, with no specific spatial variation. Of course, interpolated rain gauge measurements exhibit a better agreement to observations in the vicinity of the two TAWES stations than elsewhere. The rapid-INCA field also shows an underestimation of precipitation higher than 0.5 mm/5 min but with better results near the stations. Especially the TAWES station of Feldbach (further north) has a positive impact on the bias of rapid-INCA. Note that the larger positive bias at one location in the northern part of the area is due to erroneous measurements of the corresponding WegenerNet station.

MAE and RMSE are similar error measures and also show similar characteristics in Figure 12. With RMSE emphasizing large errors, the spatial distribution of the errors is more pronounced. Again, no significant spatial variation can be indicated for radar derived QPE, whereas interpolated TAWES station data and rapid-INCA exhibit a better performance around the Feldbach station. The TAWES station further south (Bad Gleichenberg) yields worse results which may be attributed to the topography in this region: Bad Gleichenberg is surrounded by hills to the north, east, and west (Figure 1). With the closest radars are as far as 100 km and 135 km, the large scan volumes in the areas of interest reduce the spatial variability which can be resolved in the radar measurement. The minimum visible height of 2000 m above ground adds further estimation errors for ground precipitation. But local differences cannot be attributed to local beam shielding effects (compare Figure 2b).

Figure 13 shows the skill score results for a threshold of 0.5 mm/5 min. Obviously, there is a tendency to underestimate the precipitation amounts (FBI < 1) for all components; the best results for FBI are obtained close to the TAWES station of Feldbach. TSS indicates more hits than misses (TSS closer to 1) near the stations. ETS yields best results for the rapid-INCA analysis.

To investigate the influence of the threshold on the error measures and skill scores, mean values of the error measures and skill scores have been calculated for several thresholds (Figure 14). The bias of rapid-INCA increases for increasing thresholds of the selected data. Thus, there is a pronounced underestimation of heavy precipitation events. Interpolated rain gauge measurements yield a lower negative bias compared to rapid-INCA which can be attributed to the relatively better performance near the stations, whereas rapid-INCA shows a spatially more homogenous distribution of the bias (compare Figure 12). Generally, the variation in error measures and skill scores for the TAWES station data is much higher than for rapid-INCA analysis and radar derived QPE. Averaging over the WegenerNet domain can lead to better performance of the error measures and skill scores.

Note that the MAE increases with the threshold whereas the RMSE is decreasing. This behavior indicates that large errors mostly occur for samples including light precipitation amounts (with RMSE putting higher weight on outliers). The coarse resolution of the radar data with a minimum detected signal of 11.8 dBZ (approximately 0.2 mm/h) and the reduced visibility in the target region can be reasons for the underestimation of light precipitation in rapid-INCA analyses.

For thresholds of up to 1 mm (FBI), 0.5 mm (TSS), and 0.2 mm (ETS) the skill scores show best results for rapid-INCA. At higher thresholds the TAWES stations exhibit better scores than the combined product. During heavy precipitation events, the interpolated rain gauge measurements usually overestimate the spatial precipitation amount and yield better scores than the radar derived QPE which usually underestimates the precipitation field. Additionally, the merging of radar QPE and TAWES station data consists of non-linear algorithms which cause rapid-INCA to converge to the radar QPE for heavy precipitation (due to the non-representative behavior of rain gauge measurements during convective events). As long as no hail effects are involved in the measurement, it is likely that convective rainfall intensities are underestimated in the radar QPE due to the fixed Marshall-Palmer relation, which is used to convert radar reflectivities to rainfall intensities. It has been concluded in several studies, that different rain types would need different Z-R relationships (Austin, 1987; Atlas, 1999; Steiner et al., 2003). The Marshall-Palmer relation has been found to yield good results in stratiform rain, but can fail in convective rain (Foote, 1965; and following from the findings in Austin, 1987; Steiner et al., 2004).

5 Conclusions

In the present study, the performance of short-duration, high-resolution precipitation analyses has been elaborated by means of a set of convective events and a long-term validation covering the convective season in 2011 (01 April 2011 - 30 September 2011). In order to point out the small-scale features of convective events, the dense station network of WegenerNet, which is located in the south-eastern parts of Austria (Styria), has been used as a reference.

The validation results show a general underestimation of rapid-INCA and its constituents (radar derived QPE and rain gauge measurements of TAWES). The spatial variation in error measures is highest for the interpolated TAWES station data. Results from the four selected cases in August and September 2011 show that the contribution from TAWES station interpolation can either have a positive or negative impact on the rapid-INCA skill, depending on the representativeness of the station measurements. Merging TAWES station data with radar derived QPE is able to reduce this effect, but is not able to avoid it completely. Another

reason for the underestimation might be the tendency to miss heavy precipitation with rapid-INCA.

This study indicates that the station contributions play a crucial part in the performance of the rapid-INCA analyses or, in general in any radar - gauge merging method. Depending on the prevalent synoptic situation, e.g. local convection or large scale precipitation, it may prove useful to adapt the station interpolation algorithm accordingly. Instead of a static IDW with both a fixed number of included nearest stations and a fixed exponent it could be advantageous to apply an IDW with dynamically adjusted parameters. Thus, further studies are needed to investigate the influence of IDW parameters as well as modifications in the combination algorithm on the validation results. Also an improved pre-scaling of radar QPE may be useful since radar QPE shows a strong underestimation over the whole dataset. As it has been outlined in detail already 35 years ago in Wilson and Brandes (1979) and more recently in Krajewski et al. (2010), radar QPE is prone to a number of measurement errors.

For rapid-INCA analyses, the MaxCAPPI product is used as the best available information source. As the data are only corrected for ground clutter and R-LAN, beside residual clutter, all other error sources have to be considered when radar QPE is used. Topographically complex domains will always face the problem of locally reduced radar visibilities and elevated radar locations on mountain massifs. However, the recent upgrade of the Austrian radar network to dual-pol technology provides possibilities for more sophisticated methods of quality control and data correction, which promise more accurate radar QPE products. Apart from further improvements by applying more sophisticated radar - rain gauge blending methods, the quantification of the uncertainties related to the representativeness problem is a key issue in the generation of an ensemble of precipitation analyses.

The present study reveals that the WegenerNet, which offers high-quality station measurements on very high temporal and spatial resolution, is ideally suited to further improve precipitation analyses and to assess their skill and uncertainty.

Acknowledgements

The authors thank Martin Suklitsch, Christine Gruber, and Robert Goler for fruitful discussions about scientific and operational issues, and the editor and two anonymous referees for fruitful comments that led to substantial improvements of the manuscript.

References

Atlas, D., Ulbrich, C. W., Marks Jr., F. D., Amitai, E., and Williams, C. R.: Systematic variation of drop size and radar-rainfall relation, J. Geophys. Res., 104(D6), 6155- 6169, 1999.

Austin, P. M.: Relation between Measured Radar Reflectivity and Surface Rainfall, Mon. Weather Rev., 115, 1053-1070, 1987.

Chumchean, S., Sharma, A., and Seed, A.: An Integrated Approach to Error Correction for Real-Time Radar-Rainfall Estimation, J. Atmos. Ocean. Tech., 23, 67-79, 2006.

Golding, B. W.: Nimrod: A system for generating automated very short range forecasts, Meteorol. Appl., 5, 1-16, 1998.

Foote, G. B.: A Z-R relation for mountain thunderstorms, J. Appl. Meteorol., 2, 229-231, 1966.

Goudenhoofdt, E. and Delobbe, L.: Evaluation of radar-gauge merging methods for quantitative precipitation estimates, Hydrol. Earth Syst. Sc., 13, 195–203, 2009.

Gregow, E., Saltikoff, E., Albers, S., and Hohti, H.: Precipitation accumulation analysis - assimilation of radar-gauge measurements and validation of different methods, Hydrol. Earth Syst. Sc., 17, 4109-4120, 2013.

Haiden, T. and Pistotnik, G.: Intensity-dependent parameterization of elevation effects in precipitation analysis, Adv. Geosci., 20, 33-38, 2009.

Haiden, T., Kann, A., Wittmann, C., Pistotnik, G., Bica, B., and Gruber, C.: The Integrated Nowcasting through Comprehensive Analysis (INCA) System and Its Validation over the Eastern Alpine Region, Weather Forecast., 26, 166-183, 2011.

Handcock, M. S. and Stein, M. L.: A Bayesian analysis of Kriging, Technometrics, 35**,** 403-410, 1993.

Kabas, T.: WegenerNet Klimastationsnetz Region Feldbach: Experimenteller Aufbau und hochauflösende Daten für die Klima- und Umweltforschung, Wiss. Ber. 47, document WCV-WissBer-No47-TKabas-Jan2012.pdf, Wegener Center Verlag, Graz, Austria, available at: http://www.wegcenter.at/wcv/ (last access: 15 January 2014), 2012.

Kabas, T., Foelsche, U., and Kirchengast, G.: Seasonal and annual trends of temperature and precipitation within 1951/1971-2007 in South-Eastern Styria/Austria, Meteorol. Z., 20**,** 277-289, 2011a.

Kabas, T., Leuprecht, A., Bichler, C., and Kirchengast, G.: WegenerNet climate station network region Feldbach, Austria: network structure, processing system, and example results, Adv. Sci. Res., 6**,** 49-54, 2011b.

Kaltenboeck, R.: New generation of dual polarized weather radars in Austria, in: Proceedings of the 7th European Conference on Radar in Meteorology and Hydrology (ERAD), Toulouse, France, 24 - 29 June 2012, 6 pp, 2012.

Kaltenboeck, R. and Steinheimer, M.: Radar-based severe storm climatology for Austrian complex orography related to vertical wind shear and atmospheric instability. Atmos. Res., doi:10.1016/j.atmosres.2014.08.006, 2014.

Kann, A., Haiden, H., von der Emde, K., Gruber, C., Kabas, T., Leuprecht, A., and Kirchengast, G.: Verification of operational analyses using an extremely high-density surface station network, Weather Forecast., 26, 572-578, 2011.

Kirchengast, G., Kabas, T., Leuprecht, A., Bichler, C., and Truhetz, H.: WegenerNet: A pioneering high-resolution network for monitoring weather and climate, B. Am. Meteorol. Soc., 95**,** 227-242, 2014.

Komma, J., Reszler, C., Blöschl, G., and Haiden, T.: Ensemble prediction of floods - catchment non-linearity and forecast probabilities, Nat. Hazard Earth Sys., **7,** 431-444, 2007.

Krajewski, W. F.: Co-kriging radar-rainfall and raingage data, J. Geophys. Res., 92, 9571-9580, 1987.

Krajewski, W. F., Villarini, G., and Smith, J. A.: RADAR-Rainfall Uncertainties, B. Am. Meteorol. Soc., 91, 87-94, 2010.

Marshall, J. S. and Palmer, W. M.: The distribution of raindrops with size, J. Meteorol., 5, 165 - 166, 1948.

Morin, E., Krajewski, W. F., Goodrich, D. C., Gao, X., and Sorooshian, S.: Estimating rainfall intensities from weather radar data: The scale-dependency problem, J. Hydrometeorol., 4, 782-797, 2003.

Overeem, A., Holleman, I., and Buishand, A.: Derivation of a 10-year radar-based climatology of rainfall, J. Appl. Meteorol. Clim., 48, 1448–1463, 2009.

Pereira Fo, A. J., Crawford, K. C., and Hartzell, C. L.: Improving WSR-88D Hourly Rainfall Estimates, Weather Forecast., 13, 1016–1028, 1998.

Rezacova, D. and Sokol, Z.: Results of numerical experiments with LM DWD - First attempts to verify precipitation forecast by radar derived rainfall fields (1998 flood event), COST-717 Working document WDF_02_200204_2, Brussels, 12 pp, 2002.

Rossa, A., Bruen, M., Frühwald, D., Macpherson, B., Holleman, I., Michelson, D., and Michaelides, S.: Use of Radar Observations in Hydrological and NWP Models. ESSEM COST Action 717, Office for Official Publications of the European Communities, Brussels, 292 pp, 2005.

Sattler, K. and Feddersen, H.: Limited-area short-range ensemble predictions targeted for heavy rain in Europe, Hydrol. Earth Syst. Sc., 9, 300-312, 2005.

Scheidl, D.: Improved quality control for the WegenerNet and demonstration for selected weather events and climate. Sci. Rep. No. 61, document WCV-SciRep-No61-DScheidl-Oct2014.pdf, Wegener Center Verlag, Graz, Austria, available at: http://www.wegcenter.at/wcv/ (last access: 15 January 2014), 2014.

Steiner, M., Smith, J. A., and Uijlenhoet, R.: A Microphysical Interpretation of Radar Reflectivity–Rain Rate Relationships, J. Atmos. Sci., 61, 1114-1131, 2004.

Sun, X., Mein, R. G., Keenan, T. D., and Elliott, J. F.: Flood estimation using radar and raingauge data, J. Hydrol., 239, 4–18, 2000.

Wernli, H., Paulat, M., Hagen, M., and Frei, C.: SAL - A novel quality measure for the verification of quantitative precipitation forecasts, Mon. Weather Rev., 136, 4470-4487, 2008.

Wilks, D. S.: Statistical Methods in the Atmospheric Sciences, 2nd edition. Academic Press, Burlington, MA; London, 627 pp, 2006.

Wilson, J. W. and Brandes, E. A.: Radar Measurement of Rainfall - A Summary, B. Am. Meteorol. Soc., 60, 1048-1058, 1979.

Wittmann, C., Haiden, T., and Kann, A.: Evaluating multi-scale precipitation forecasts using high resolution analysis, Adv. Sci. Res., 4**,** 89-98, 2010.

Wussow, G.: Untere Grenzwerte dichter Regenfälle. Meteorol. Z. 39, 173–178, 1922.

Table 1. Overview of the WegenerNet data quality-control (QC) layers.

QC layer	Description
0: check regarding station operation	Check if station is currently in operations
1: check of data availability	Check if expected sensor data values are available
2: check of sensor functioning	Check if measurement value exceeds permitted range of technical sensor specifications
3: check of climatological plausibility	Check if measurement value exceeds plausibly set maximum climatological bounds
4: check of temporal variability	Check if measurement value shows too high or too little variation (“jumps”, “constancy”)
5: check of intra-station consistency	Check if measurement value is not properly consistent with related parameters
6: check of inter-station consistency	Check if measurement value deviates too much from values at neighbor stations
7: check against external reference	Check (for pressure) if measurement value deviates too much from ZAMG reference

Table 2. Skill scores used for validation (Wilks, 2006). See also WMO Joint Working Group on Forecast Verification Research, e.g.: http://www.cawcr.gov.au/projects/verification/

	ETS (Equitable Threat Score)	True Skill Score (TSS)	Frequency bias Index (FBI)
Range	-1/3 to 1, 0: no skill	-1 to 1, 0: no skill	0 to ∞
Perfect score	1	1	1
Answers the question:	How well did the forecast "yes" events correspond to the observed "yes" events?	How well did the forecast separate the "yes" events from the "no" events?	How did the forecast frequency of "yes" events compare to the observed frequency of "yes" events?

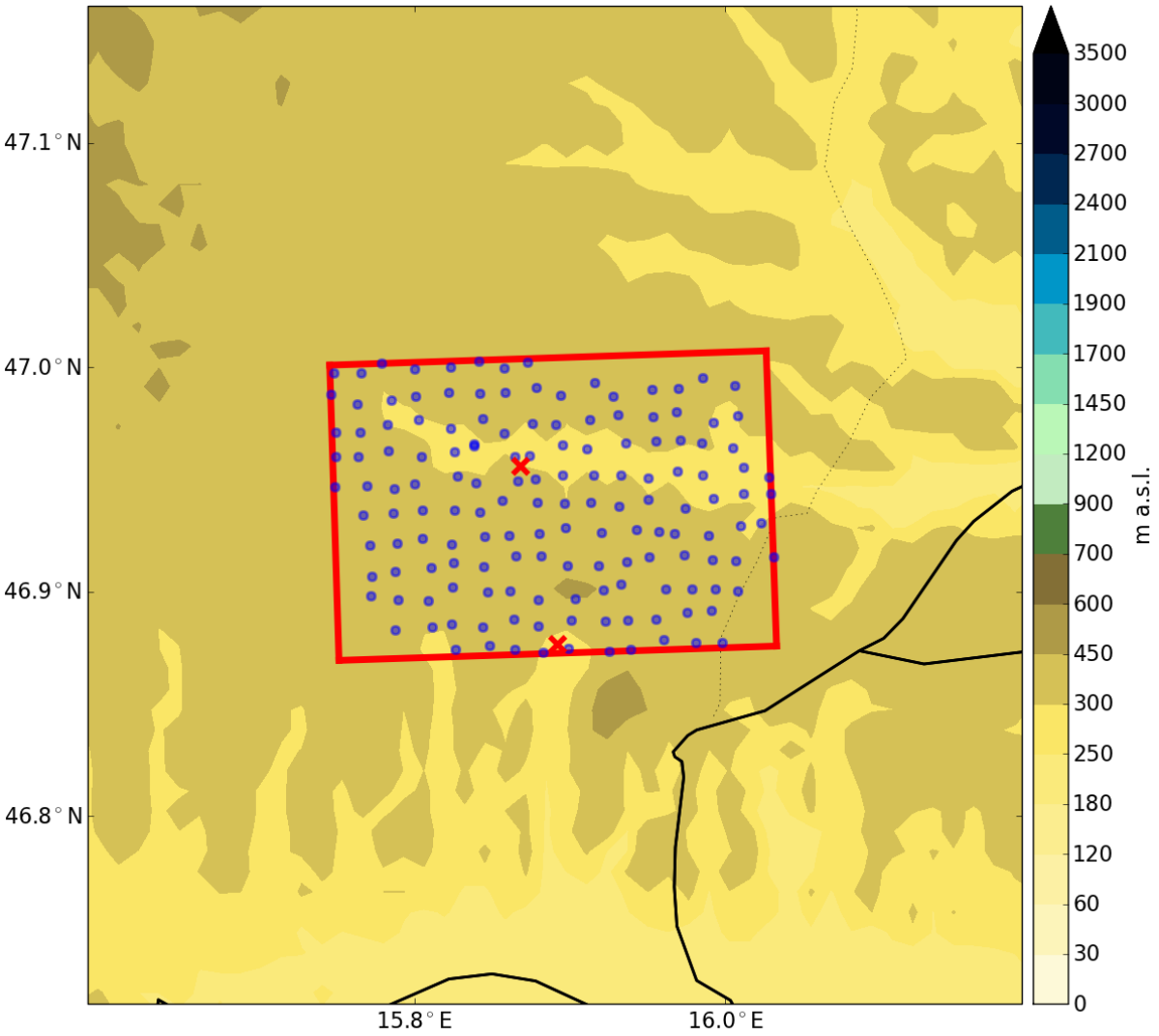

Figure 1. rapid-INCA topography in the WegenerNet region. Blue circles represent WegenerNet stations, red crosses are the TAWES stations (Teilautomatische Wetterstationen) Feldbach (north) and Bad Gleichenberg (south) of ZAMG.

(a)

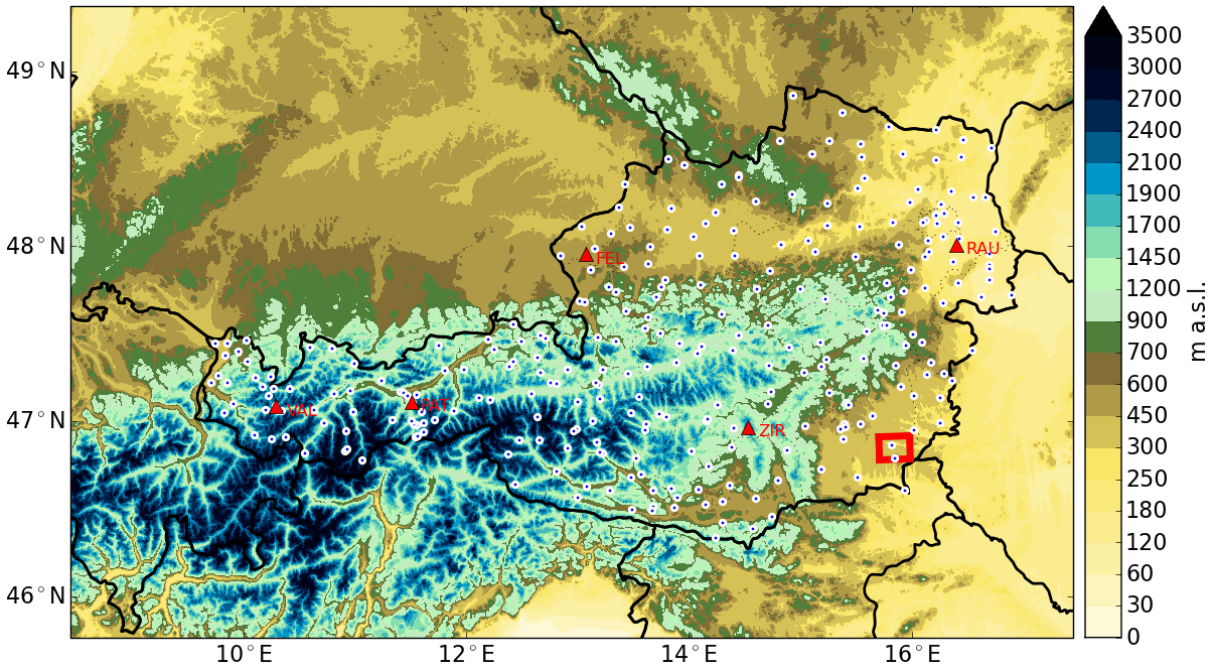

(b)

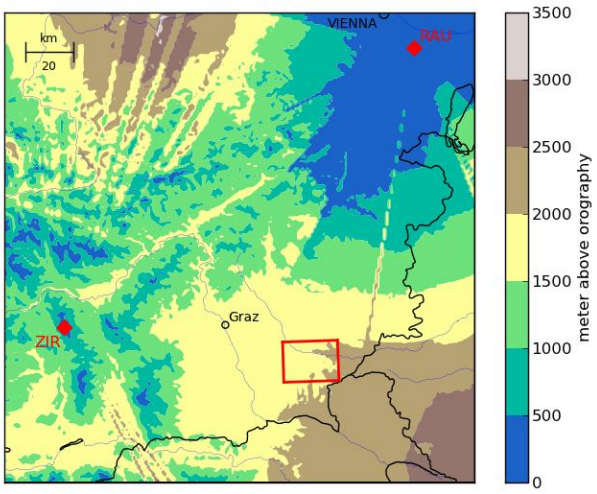

Figure 2. (a) Operational rapid-INCA domain, orography and rain gauge stations (TAWES) measuring precipitation in 5-minute intervals (white/blue dots). Additionally, the locations of the five radars are marked (red triangles) as well as the WegenerNet region (red square).

(b) Relative height of the lowest available radar beam above orography, in combination with the location of the WegenerNet (red box) and the locations of the radars Rauchenwarth (RAU) and Zirbitzkogel (ZIR) (red diamonds).

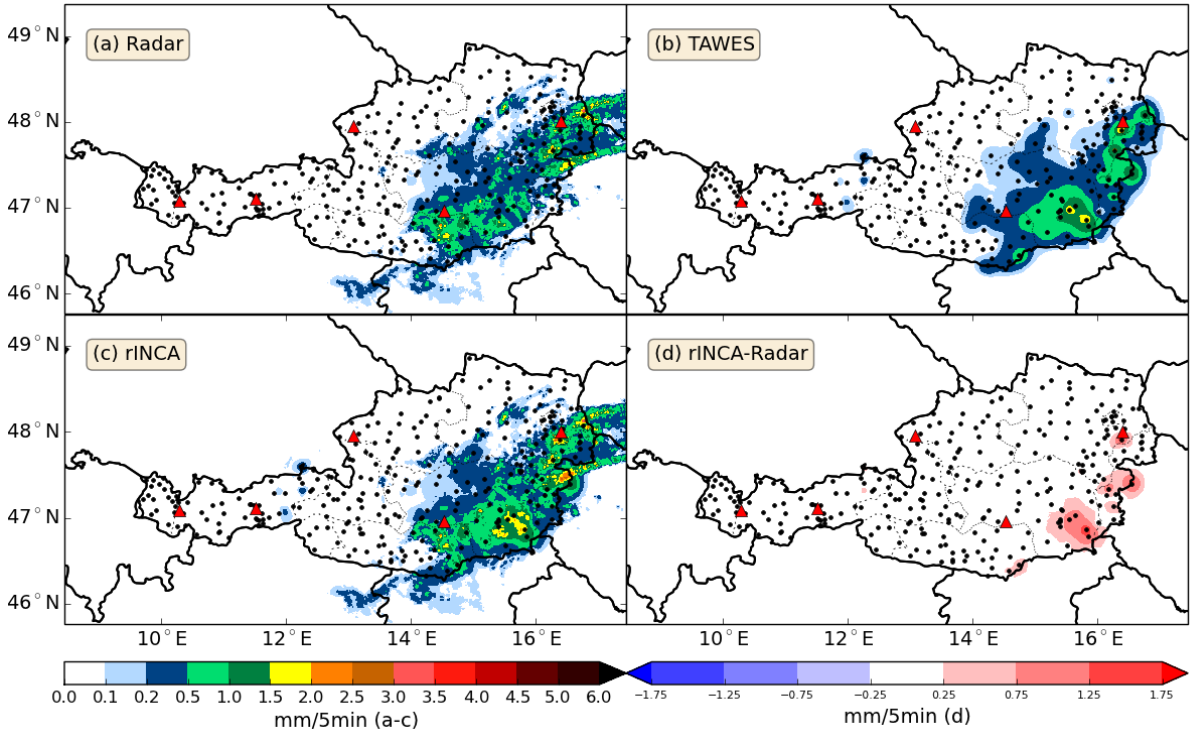

Figure 3. Example of a 5-minute precipitation analysis (rapid-INCA) based on the combination of rain gauge data and radar derived QPE on 13 September 2014, 02:40 UTC. (a) scaled radar field, (b) interpolated rain gauge measurements (TAWES), (c) final rapid-INCA precipitation analysis and (d) difference between rapid-INCA and radar derived QPE.

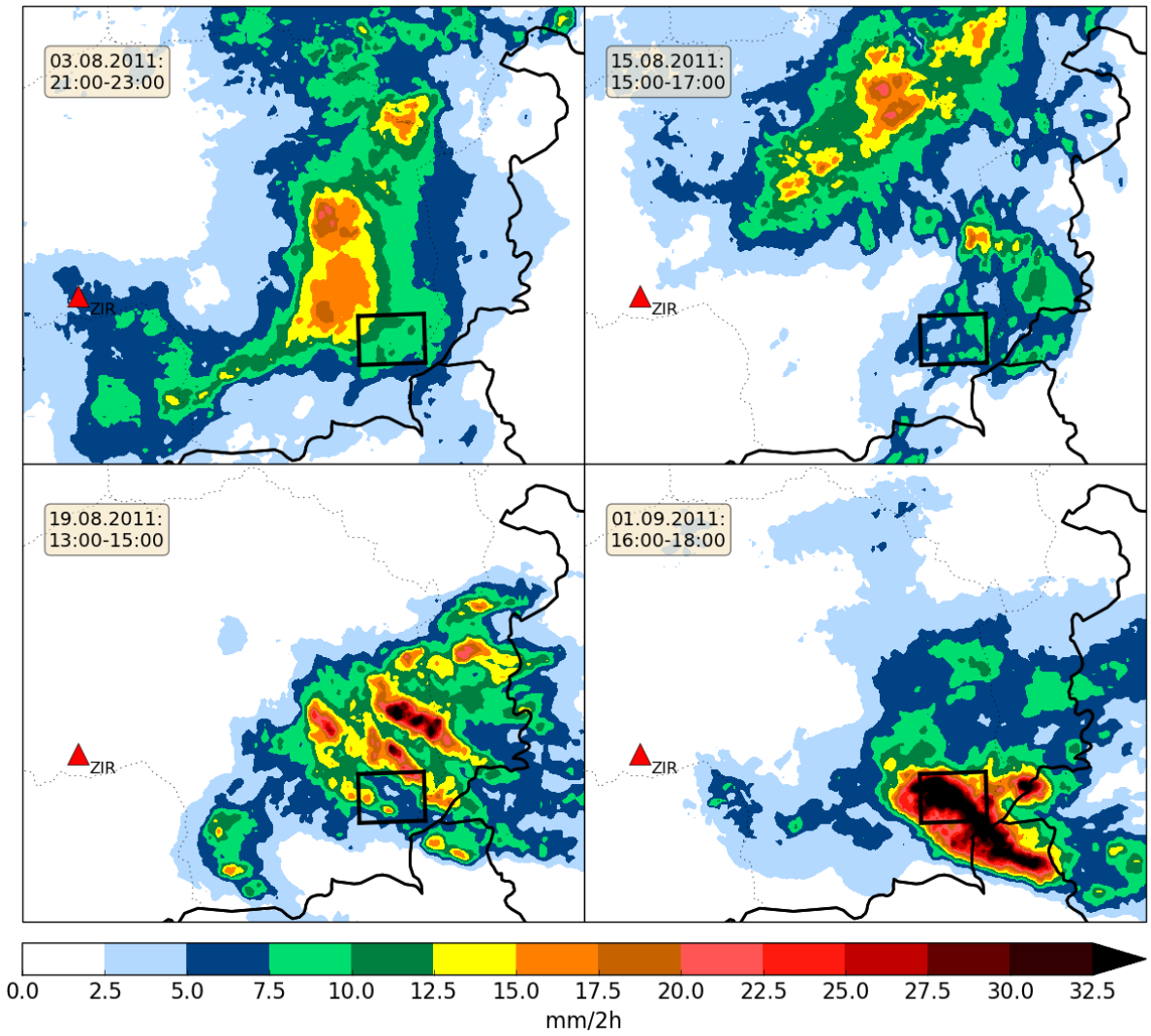

Figure 4. 2-hour precipitation accumulations of the 5-minute rapid-INCA analyses on four days (top left: 03 August 2011, top right: 15 August 2011, bottom left: 19 August 2011, bottom right: 01 September 2011) in the respective time spans. The WegenerNet region is marked by a small black rectangle, the red triangle represents the radar (Zirbitzkogel) within this zoom.

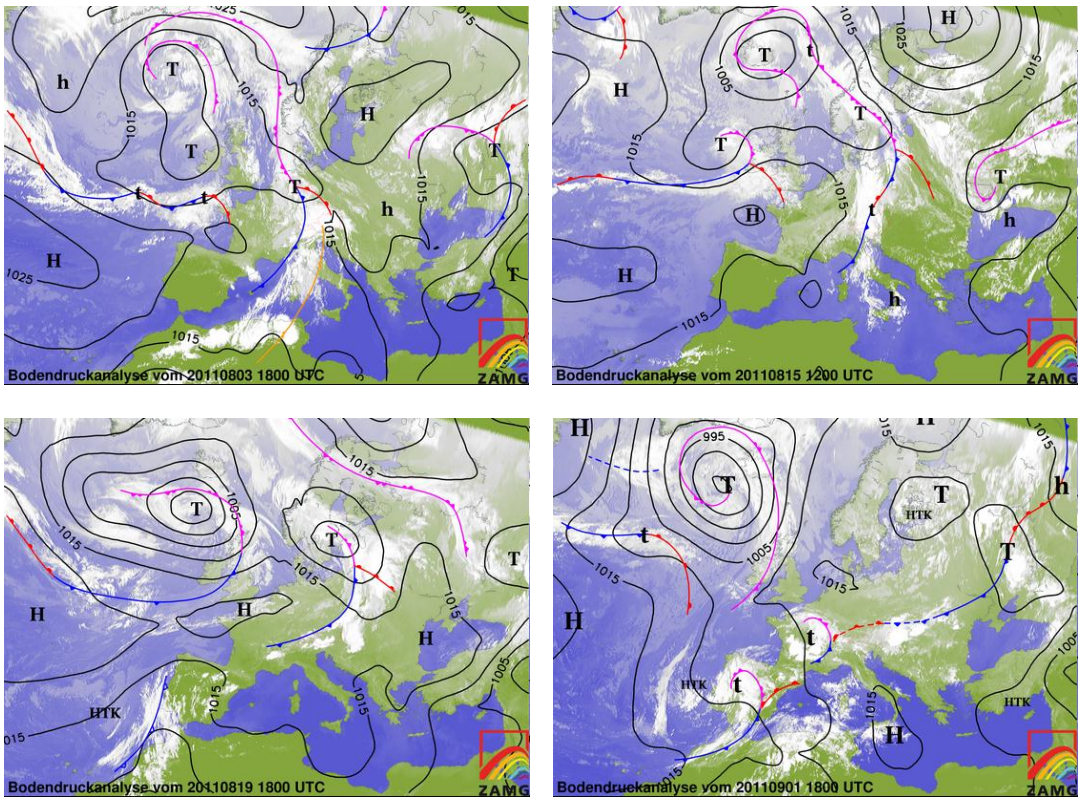

Figure 5. Satellite image, surface pressure analysis and frontal zones on the four selected days. Top left: 03 August 2011, 18:00 UTC; top right: 15 August 2011, 12:00 UTC; bottom left: 19 August 2011, 18:00 UTC; bottom right: 01 September 2011, 18:00 UTC.

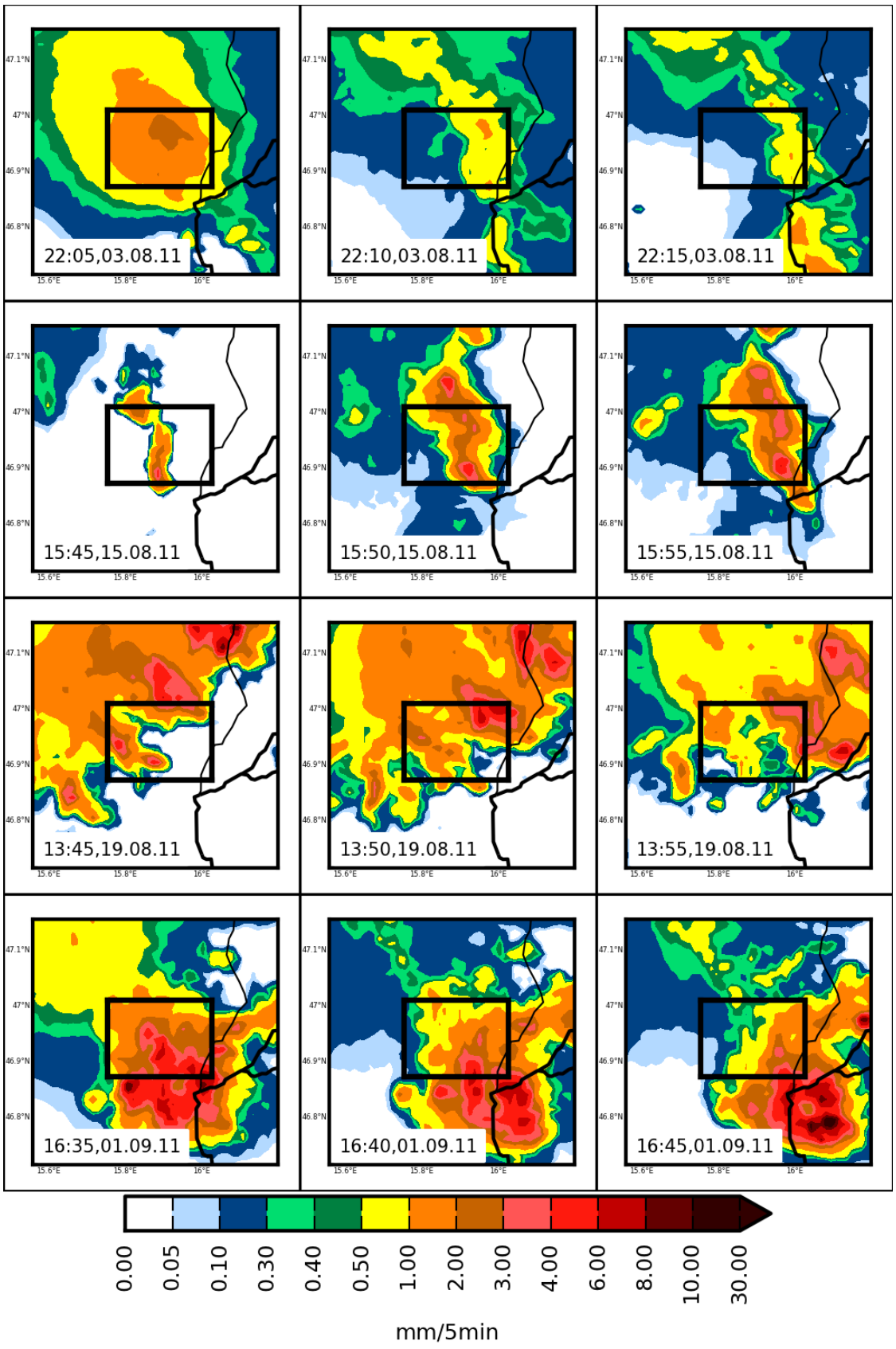

Figure 6. Spatio-temporal distribution of rapid-INCA precipitation (mm/5min) in the region of the WegenerNet indicated by the black rectangle (time is given in UTC).

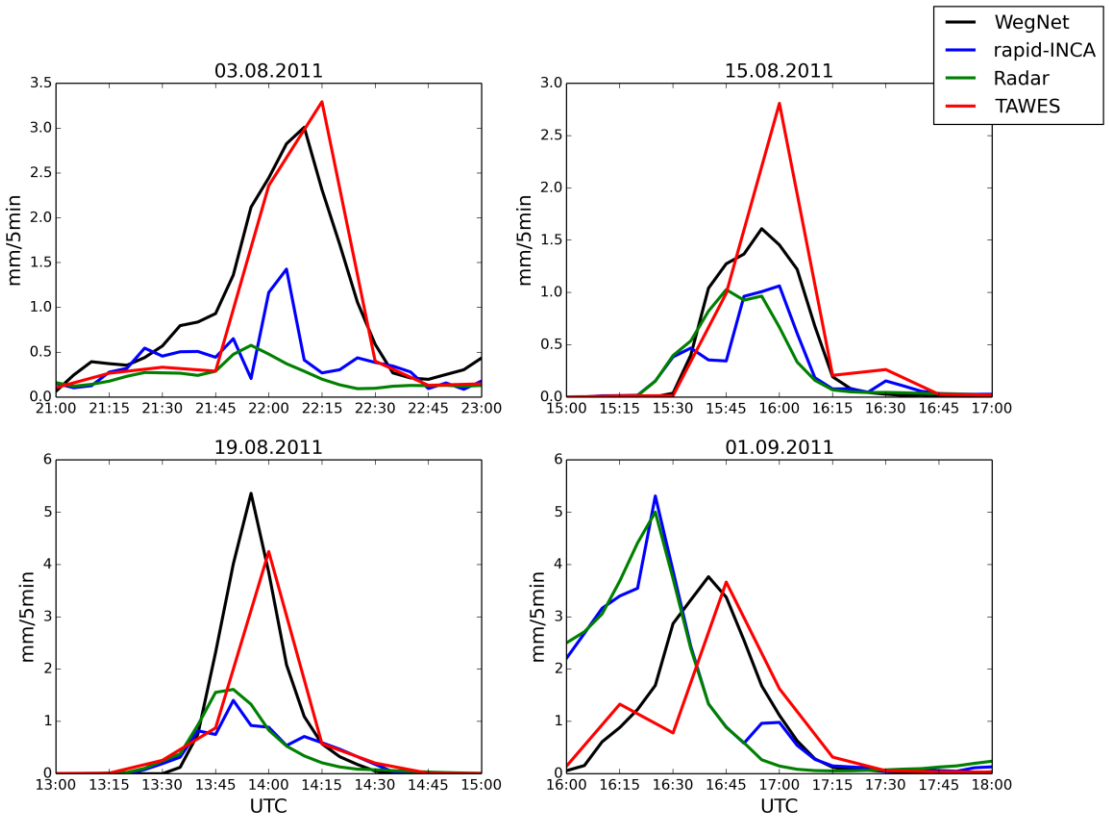

Figure 7. Temporal evolution of precipitation rates for WegenerNet (WegNet), rapid-INCA, radar derived QPE (Radar), and TAWES station and four selected cases.

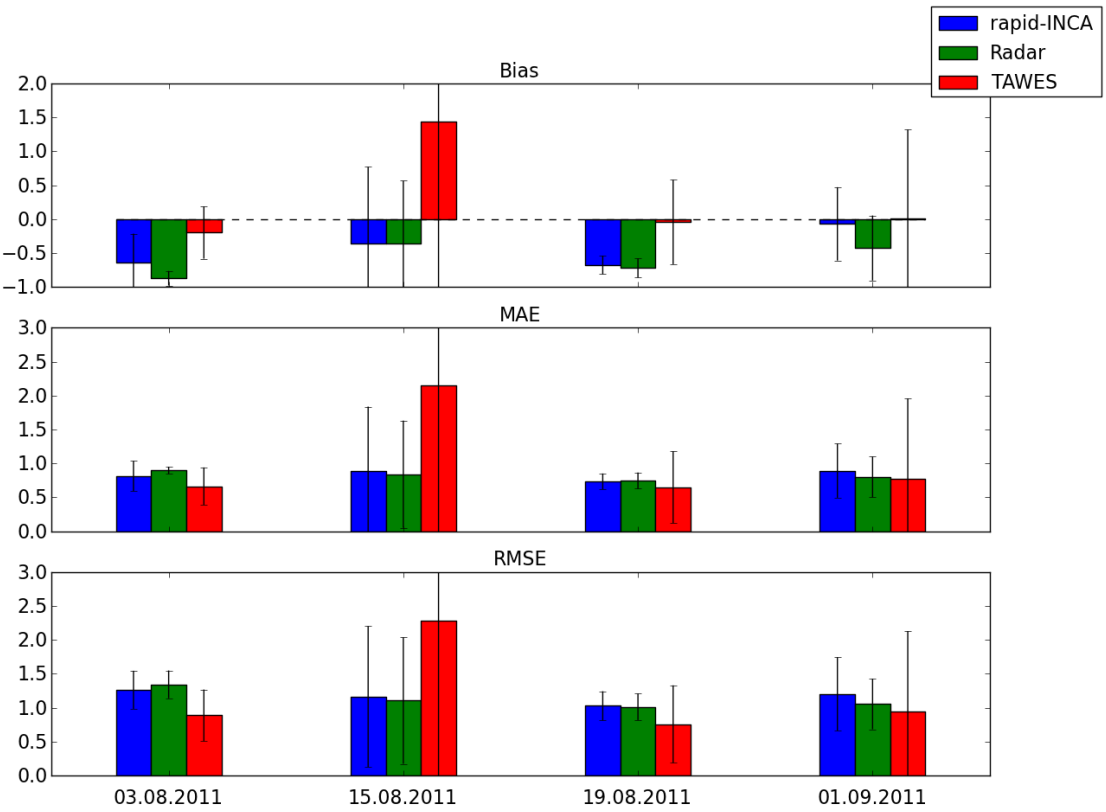

Figure 8. Relative bias, MAE, and RMSE (weighted by the mean observed precipitation of WegenerNet). Values have been computed for each of the WegenerNet stations (151 stations) and then averaged over space. Error bars represent the standard deviation of obtained verification measures at each WegenerNet station.

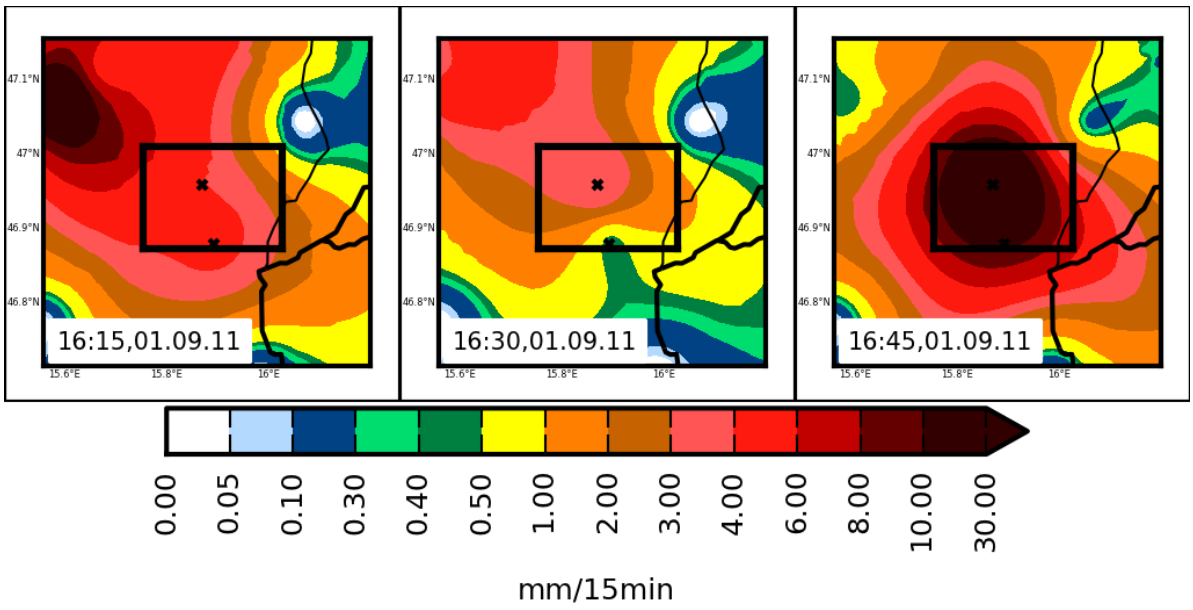

Figure 9. Spatio-temporal distribution of 15-minute interpolated TAWES station measurements (mm/15min) on 01.09.2011 between 16:15 and 16:45 UTC (region of WegenerNet is shown by the black rectangle and the two TAWES stations of ZAMG are marked with a cross).

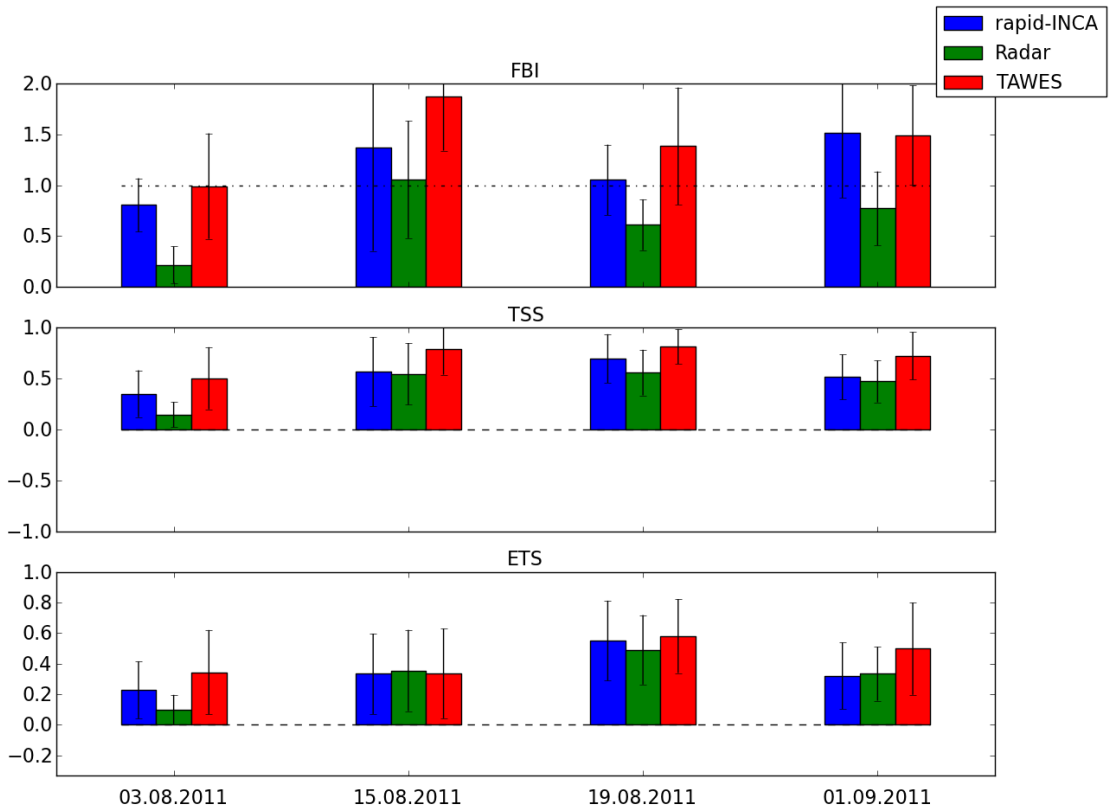

Figure 10. Skill scores for threshold of 0.5 mm/5 min. Scores are computed at each WegenerNet station and then averaged over space. Error bars indicate the standard deviation of the scores.

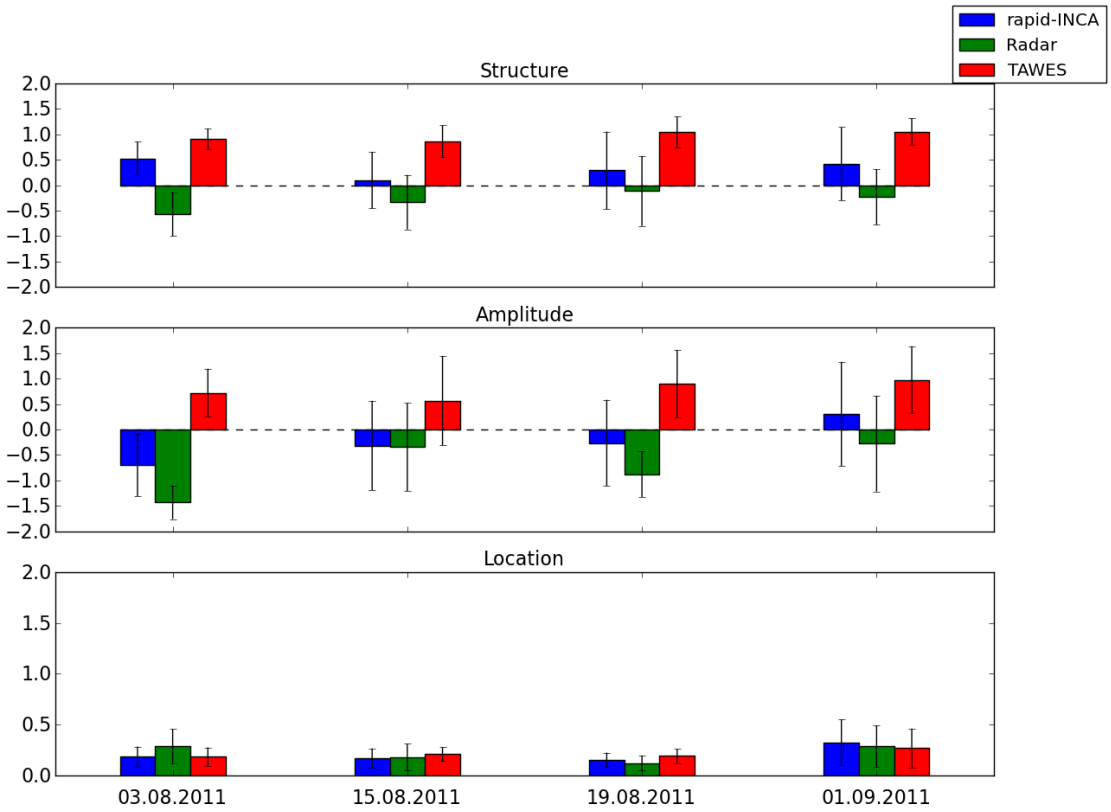

Figure 11. Structure, Amplitude, and Location computed for each time step within the 2-hour intervals at each date and subsequently averaged. Error bars indicate the standard deviation of S, A, L time series

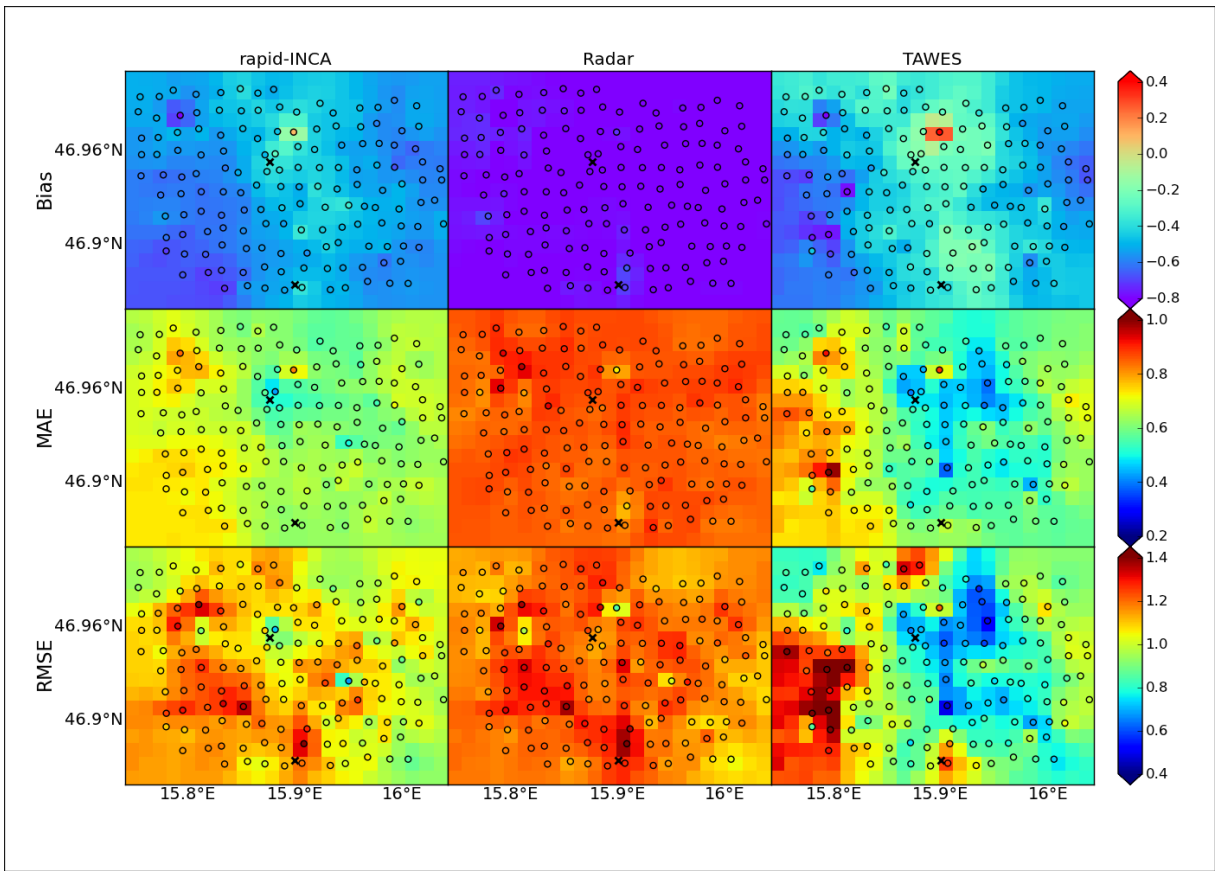

Figure 12. Relative bias, MAE, and RMSE for rapid-INCA, radar and TAWES stations at each WegenerNet station. Only those data points are included where the WegenerNet station measured more than 0.5 mm/5 min. Circles represent exact values at the WegenerNet stations, the image is obtained by IDW interpolation to the INCA grid

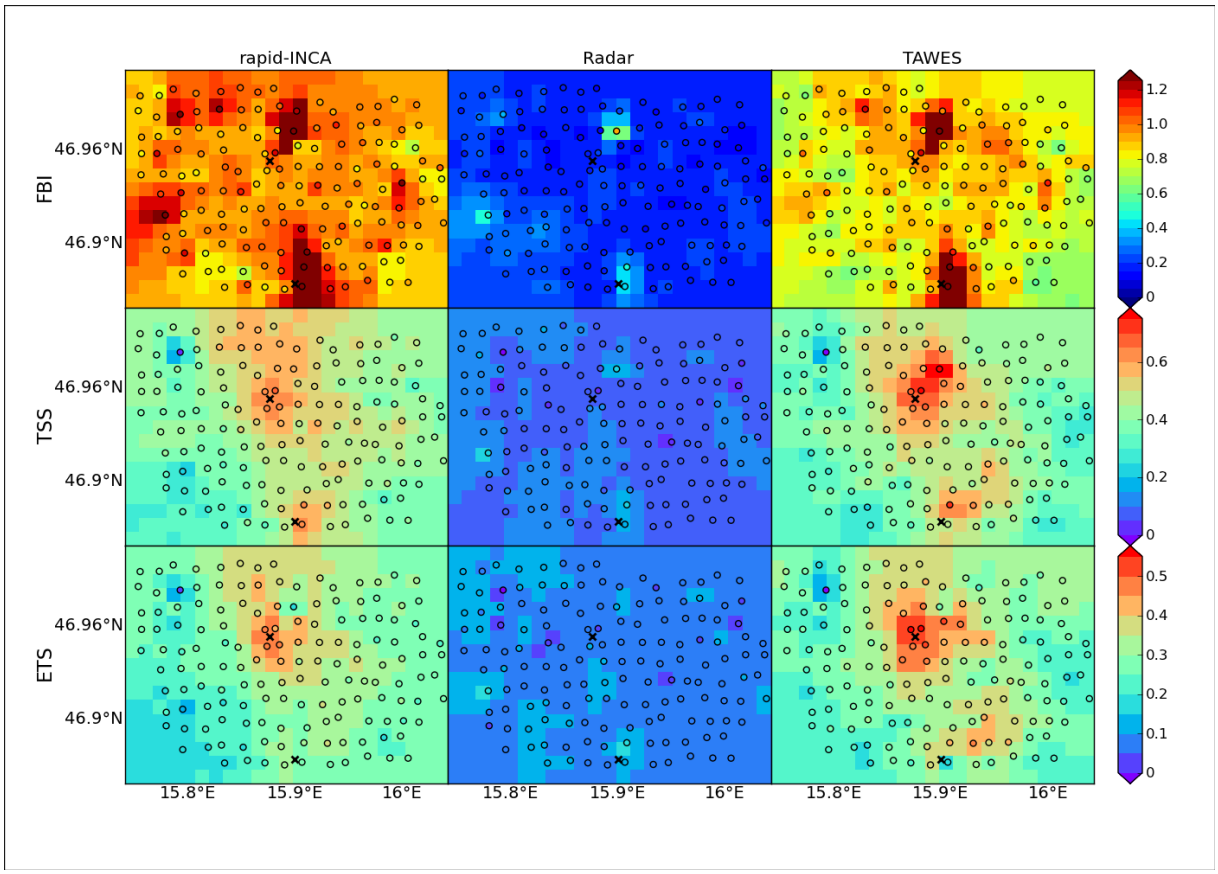

Figure 13. Skill scores for rapid-INCA, radar, and TAWES stations at each WegenerNet station. Circles represent the exact values; the image is obtained by interpolation to the INCA grid

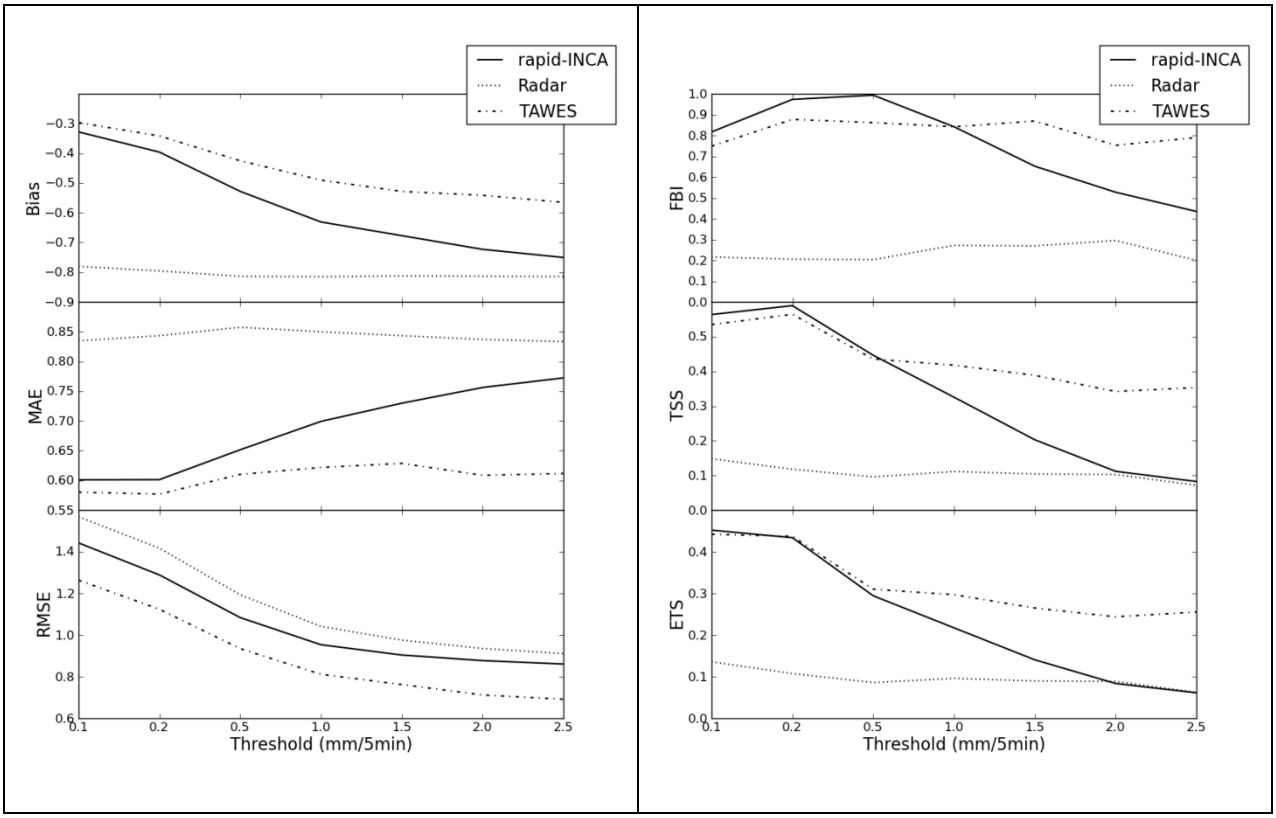

Figure 14. Mean relative error scores (bias, MAE, RMSE) and mean skill scores (FBI, TSS, ETS) computed for several thresholds.